DENTAL MATERIALS 35 (2019) 1776–1790

Available online at www.sciencedirect.com

ScienceDirect

journal homepage: www.intl.elsevierhealth.com/journals/dema

High-translucent yttria-stabilized zirconia ceramics are wear-resistant and antagonist-friendly

Fei Zhang[a,b,c,*], *Benedikt C. Spies*[d], *Jef Vleugels*[c], *Helen Reveron*[a], *Christian Wesemann*[d], *Wolf-Dieter Müller*[d], *Bart van Meerbeek*[b], *Jérôme Chevalier*[a]

[a] *Université de Lyon, INSA-Lyon, MATEIS UMR CNRS 5510, 7 Avenue Jean Capelle, 69621 Villeurbanne Cedex, France*

[b] *KU Leuven (University of Leuven), Department of Oral Health Sciences, BIOMAT -Biomaterials Research Group & UZ Leuven (University Hospitals Leuven), Dentistry, Kapucijnenvoer 7 blok a, B-3000 Leuven, Belgium*

[c] *KU Leuven, Department of Materials Engineering, Kasteelpark Arenberg 44, B-3001 Heverlee, Belgium*

[d] *Charité - Universitätsmedizin Berlin, Corporate member of Freie Universität Berlin, Humboldt-Universität zu Berlin, and Berlin Institute of Health, Department of Prosthodontics, Geriatric Dentistry and Craniomandibular Disorders, Aßmannshauser Str. 4-6, Berlin, Germany*

ARTICLE INFO

Keywords:
Yttria-stabilized zirconia
Yttria content
Lithium-disilicate glass-ceramic
Two-body wear
Fracture toughness

ABSTRACT

Objectives. To evaluate two-body wear of three zirconia ceramics stabilized with 3, 4 and 5 mol% yttria and to compare their wear behavior with that of a lithium-disilicate glass-ceramic.

Methods. Sixteen rectangular-shaped specimens made from three grades of zirconia ceramics and a lithium-disilicate glass-ceramic were polished and dynamically loaded in a chewing simulator (2 kg vertical load, 2.1 Hz) under water at 90 °C for 1.2×10^6 cycles (about 7 days) in the ball-on-plate mode against steatite antagonists. Surface roughness was measured before and after wear testing. Wear tracks were scanned with a non-contact 3D profilometer and super-impositions were used to determine wear loss of the antagonists. Wear surfaces were imaged by SEM. XRD and micro-Raman spectroscopy were used to characterize phase transformation and stress status in the worn and unworn areas of the zirconia ceramics.

Results. Independent of fracture toughness, strength and aging-susceptibility, the three zirconia ceramics showed a similar and limited amount of wear (~10 μm in depth) and were more wear-resistant than the lithium-disilicate glass-ceramic (~880 μm in depth). Abrasive wear without obvious cracks was observed for all investigated zirconias, whereas the glass-ceramic with a lower fatigue threshold and high susceptibility to surface dissolution exhibited significant abrasion, fatigue and corrosion wear. All three zirconia ceramics yielded a lower antagonist wear than the glass-ceramic and no significant differences were found between the zirconia ceramics.

* *Corresponding author at*: KU Leuven (University of Leuven), Department of Oral Health Sciences, BIOMAT -Biomaterials Research gGroup & UZ Leuven (University Hospitals Leuven), Dentistry, Kapucijnenvoer 7 blok a, B-3000 Leuven, Belgium.
E-mail address: fei.zhang@kuleuven.be (F. Zhang).

https://doi.org/10.1016/j.dental.2019.10.009

Significance. In the context of this study, high-translucent zirconia ceramics stabilized with a higher yttria content, recently introduced in the dental field, were as wear-resistant and antagonist-friendly as conventional high-strength zirconia and suitable for monolithic restorations.

1. Introduction

The excellent mechanical properties and biocompatibility of zirconia, associated with the advances of CAD/CAM technologies, have led to an increasing popularity of this material for dental restorations [1,2]. Zirconia can be (meta)stabilized at room temperature by alloying with various dopants and phase transformation toughening, which leads to improved strength, depends on the type and the amount of stabilizer [2–4]. Conventional dental zirconia is usually referred to as 'high-strength' (~1000 MPa) and generally contains 3 mol% yttria; it is often called 3Y-TZP (3 mol% Yttria-stabilized Tetragonal Zirconia Polycristal). Nevertheless, 3Y-TZP restorations have a relatively poor translucency and veneering with a glass-ceramic is often necessary, even though improvements have been achieved in the recent years [5,6]. In order to avoid the early issues of chipping of veneering porcelain in bi-layered restoration systems [7] and to enable less invasive preparation of dental hard tissues due to adhesive luting with light-curing composite cements [8,9], the trend towards monolithic ceramic restorations is clear, increasing the requirement of high-translucent zirconia ceramics. The most robust method to improve the translucency of yttria-containing zirconia ceramics is to increase the yttria content by introducing more optically isotropic cubic phase zirconia and less birefringent tetragonal zirconia, along with a minimization of light scattering by secondary phases such as alumina particles and porosities [5,10,11]. Zirconia ceramics stabilized with higher yttria contents like 4 or 5 mol% have therefore been applied recently by dental manufacturers [5,6].

In replacement of dental hard tissues, restorations have the function of providing a hard surface layer against wear. Wear scars and facets are also often the clinically observed initiation sites for fatigue failures originating at the occlusal surface of ceramic restorations [12]. Ideal dental restorative materials need to be not only wear-resistant but also have to match with the opposing antagonist without causing excess antagonist wear. The wear behavior of high-strength 3Y-TZP ceramics provided by different manufacturers with different microstructural features has been extensively investigated [13–19]. Today, there is no doubt about their high wear resistance with very limited/negligible wear traces found after wear tests in chewing simulators [14,15,18,19], and no complaints reported in clinical observations for zirconia wear [20–22]. Due to the high hardness of zirconia ceramics (~12 GPa for fully dense 3Y-TZP), the antagonist wear against zirconia restorations was initially questioned especially for monolithic restorations [23–25]. However, with the developments and the wider use of zirconia restorations, many studies have now proven that 3Y-TZP zirconia ceramics, when their surfaces were adequately finished, are very wear-friendly to the opposing dentition amongst various dental materials [13,14,17]. Polished zirconia shows the least antagonist wear compared to sandblasted, ground, glazed and veneered surfaces [14,26–30].

To the best of the authors' knowledge, the two-body wear behaviour under oral-simulated conditions of high-translucent zirconia ceramics stabilized with higher yttria contents has been rarely studied. A very recent study showed that 3 and 5 mol% yttria-stabilized zirconia had a similar sliding wear behavior when using a ball-on-flat tribometer testing configuration against a zirconia antagonist [31]. Another study however showed that the fracture toughness and grain size significantly influenced the wear resistance of zirconia ceramics when subjected against hardmetal or zirconia balls in dry unlubricated conditions [32,33]. Studies comparing the wear behavior of different restorative materials (ceramics, including zirconia, lithium-disilicate and leucite glass-ceramics, glass-infiltrated zirconia/alumina, feldspar and polymer-infiltrated ceramics, as well as various dental composites) revealed that the materials with high strength, toughness and fatigue crack-growth resistance showed low material and/or opposing antagonist wear [12,14,15,17–19,31,34–37]. Increasing the yttria content is known to lower the fracture toughness and strength of zirconia ceramics [5,6,10]. The aging susceptibility of yttria-stabilized zirconia can be also decreased by increasing the yttria content. The hydrothermal aging of zirconia induces the tetragonal to monoclinic phase transformation and can roughen the surface of the zirconia component along with the formation of surface and subsurface micro-cracks [38–40], which may then cause detrimental consequences on the wear rate of the opposing counterface as observed for orthopedic implants [41]. Investigating the two-body wear performance of these new high-translucent zirconia stabilized with different amounts of yttria is therefore important.

The aim of this work is to investigate whether the physical and microstructural variations associated with the increased yttria content have a significant influence on the two-body wear performance of zirconia ceramics. The results were compared to those of a representative lithium-disilicate glass-ceramic, another type of frequently used dental ceramic for monolithic restorations. The null hypothesis of this study was that the high-translucent zirconia ceramics stabilized with higher yttria contents would show a different wear behavior than 3Y-TZP ceramics due to different fracture toughness and aging susceptibility.

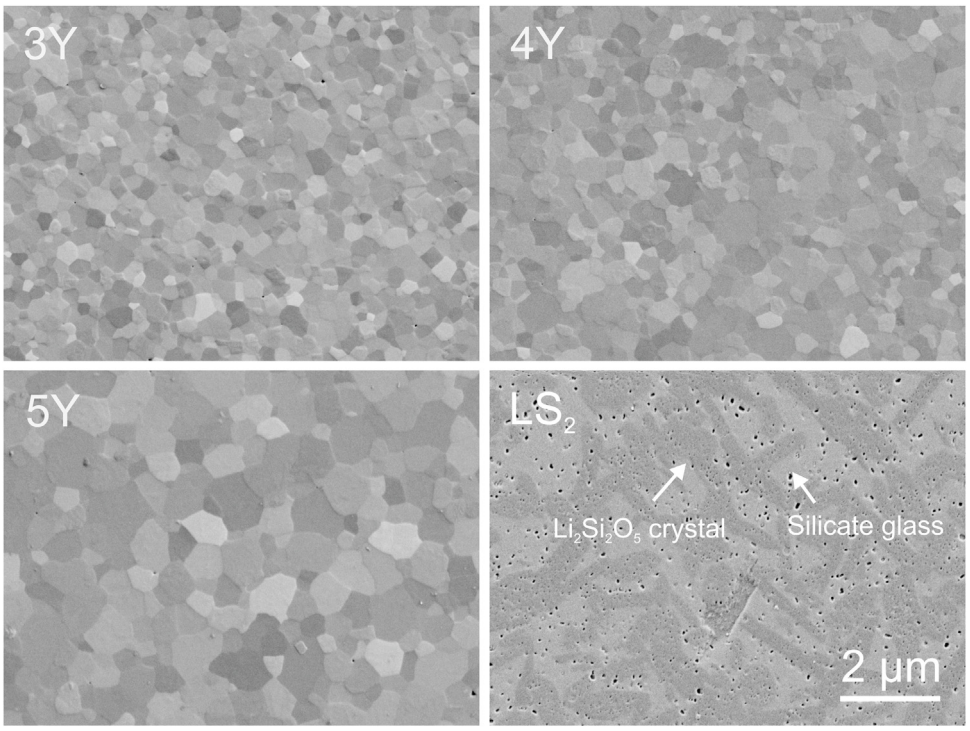

Fig. 1 – Secondary electron SEM images of the investigated materials following as-polished conditions without any etching (neither thermal for zirconia ceramics, nor chemical for LS2).

2. Materials and methods

2.1. *Materials*

Three zirconia ceramics doped with 3, 4 and 5 mol% yttria and one lithium-disilicate glass-ceramic were used. Zirconia ceramics were in-house prepared from commercially available powders (Zpex, Zpex4 and ZpexSmile, Tosoh, Tokyo, Japan). The powders were shaped by uniaxial pressing, following by cold isostatic pressing at 300 MPa for 3 min. Pressed green bodies were debinded as suggested by Tosoh (0.5 °C/min heating rate to 300 °C for 5 h and 0.5 °C/min heating rate to 700 °C for 1 h), pre-sintered at 1000 °C for 1 h and pressureless sintered at 1450 °C for 2 h in air at the heating and cooling rate of 5 °C/min, allowing all materials to be fully dense. The zirconia ceramics made from Zpex, Zpex4 and ZpexSmile contained 3, 4 and 5 mol% yttria, are referred to as '3Y', '4Y' and '5Y' throughout the text. Lithium-disilicate glass ceramic samples (referred to as 'LS_2') were cut from commercially available IPS e.max CAD blocks (IPS e.max CAD HT A2, Ivoclar Vivadent, Schaan, Liechtenstein; 'HT' = high translucency) and subjected to a crystallization firing process (850 °C for 10 min at heating rate of 30 °C/min) following the manufacturer's instructions in a Programat P300 (Ivoclar Vivadent) vacuum ceramic oven. Rectangular-shaped specimens ($10 \times 20 \times 3\,mm^3$) were finally cut from the sintered zirconia plates (approx. $22 \times 60 \times 3\,mm^3$) and the crystallized LS_2 block of approx. $18 \times 40 \times 3\,mm^3$. All ceramic specimens were mechanically polished using 15, 6, 3, 1 and 0.5 µm diamond polishing suspensions in sequence for wear testing.

The microstructure, phase composition and mechanical properties of the materials investigated are shown in Fig. 1 and Table 1, respectively. The Vickers hardness was measured by the indentation method using a micro-hardness tester (Model FV-700, Future-Tech Corp., Tokyo, Japan) with a load of 10 kg (n = 10/each grade) applied for 10 s. Details of the investigations on the phase composition, microstructure, bending strength together with the fracture toughness of exactly the same samples used in this study were reported elsewhere [6].

2.2. *Wear testing with chewing simulator*

All rectangular-shaped specimens (n = 4 per group) were ultrasonically cleaned in ethanol and embedded into prefabricated brass sample holders using a fast curing, cold polymerizing three-component resin based on modified polyester (Technovit 4000; Kulzer, Leipzig, Germany). The specimens were mounted in a computer-controlled dual-axis chewing simulator (CS-4.8, SD Mechatronik, Feldkirchen-Westerham, Germany). The wear test configuration is shown in Fig. 2 and the parameters used are presented in Table 2. The wear procedure was performed in distilled water at 90 °C [42]. The circular movement (circle diameter of 3 mm) of the antagonist/indenter (polished steatite ball with a diameter of 6 mm; n = 4 per group; CeramTec, Plochingen, Germany) loaded with a weight of 2 kg, resulted in a contact trace of 2.8 mm on the specimen surface with a potential intrusion depth due to wear up to 1 mm. The speed set at 20 mm/s resulted in a dynamic loading frequency of 2.1 Hz. During the loading period, all samples were examined twice a day. Since the intrusion depth of the antagonist was set at 1 mm, when intrusion due to

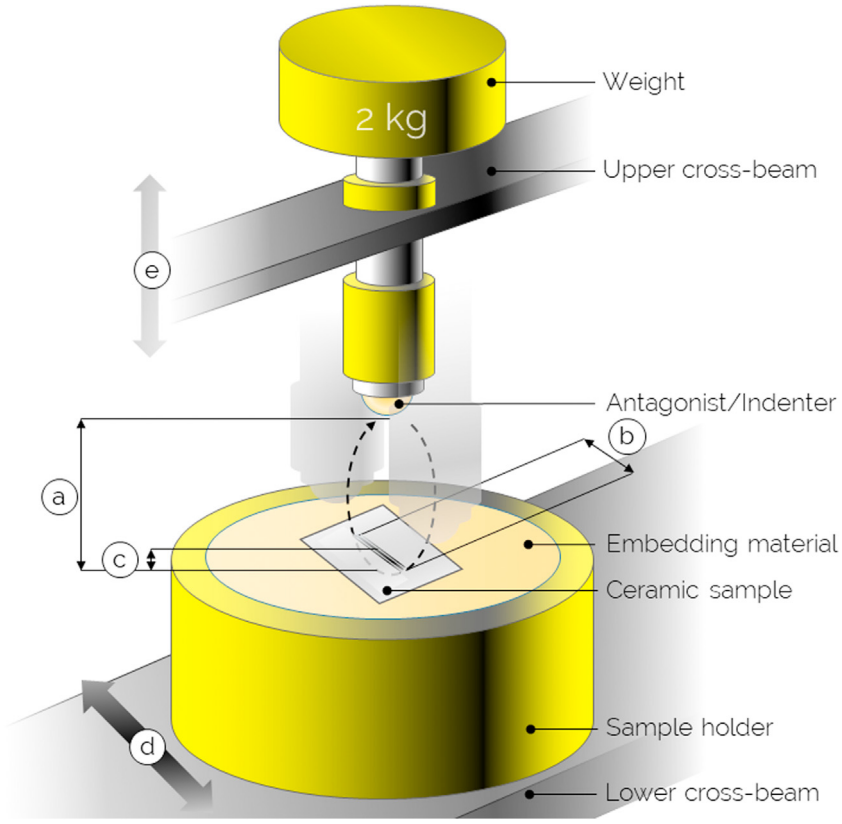

Fig. 2 – Illustration of the ball-on-plate wear testing configuration and the test parameters (a–e) are presented in Table 2.

wear of the system came close to this value, it reached the threshold of the ongoing distance measuring system and the intrusion-depth of the antagonist was re-adjusted by lowering its position to guarantee ongoing wear of the substrate. In case of water loss due to vaporization, a pump was connected with the system of all 8 chambers that refills these connected chambers to a predefined level of distilled water. Seven days were needed for applying 1.2×10^6 loading cycles. The total abrasion of the system (antagonist and ceramic specimen) were recorded by the distance measurement of the chewing simulator during the tests and the average value from 4 samples was plotted.

It is important to note that the rationale behind applying 90 °C water was to simultaneously investigate the effect of hydrothermal aging and cyclic wear. The 1.2 million cycles are generally recognized to be equivalent to 5-year function in the mouth [43]. For the aging simulation, using the Arrhenius trend with the extrapolation down to body temperature and assuming an activation energy of 100–110 kJ mol^{-1} for the zirconia phase-transformation reaction by hydrothermal aging [44], the 90 °C hydrothermal treatment in a given 7-day period was calculated to simulate 5–10 years of aging at body temperature (37 °C).

2.3. *Characterizations*

The surface roughness of each specimen was evaluated before (i.e. pristine surface) and after 1.2 million wear cycles (on worn trace) using a profilometer (Perthen Perthometer S6P, Mahr, Göttingen, Germany). Ten measurements of each specimen surface were recorded with a cut-off length of about 5.6 mm for pristine surfaces and 1.75 mm for worn surfaces, evaluation length of 0.8/0.25 mm (pristine and worn), resolution of 0.1 μm and speed of 0.5/0.1 mm/s (pristine and worn). R_a (average roughness) and R_z (average distance between the highest peak and the lowest valley) were determined. Note that throughout this article, pristine surface was referred to the polished surface that did not undergo wear tests; while worn and unworn areas were from the samples that underwent the wear tests and were referred to the loaded/aged and aged surface, respectively.

Three-dimensional wear tracks on the ceramic specimen were scanned using a 3D digital microscope (Keyence VHX-6000, Osaka, Japan) with a scanning step size of 20 μm in the x/y axes and 2 μm in the z axis (1 μm resolution of stage movement in x/y directions and 1.98 μm resolution in z axis using a 500× magnification). Wear losses (maximum wear depth, area and volume) were evaluated using the built-in software (VHX-6000_950F). The wear losses of antagonists were quantified by 3D-scanning the antagonistic steatite balls with a non-contact optical coordinate measuring microscope (InfiniteFocus, Alicona Imaging, Raaba, Austria) using a 10x magnification (0.4 μm resolution in z-axis and 3.46 μm resolution in lateral dimension). For evaluation, the datasets were exported as STL files with an edge length of 2 μm and superimposed with a scan of a new steatite ball

Table 1 – Phase composition and mechanical properties of the ceramics investigated [5,6,61].

	Phase fraction[1] (%)		Grain size[1] (μm)	Hardness, HV_{10}[2] (GPa)	E-modulus[1] (GPa)	Flexural strength[1] (MPa)	Fracture toughness[1] ($MPa \cdot m^{1/2}$)
	t-ZrO_2	c-ZrO_2					
3Y	87 ± 2	13 ± 2	0.30 ± 0.01	12.7 ± 0.2[a]	200–210	908 ± 44[a]	5.1 ± 0.3[a]
4Y	63 ± 4	37 ± 4	0.36 ± 0.02	12.8 ± 0.2[a]	200–210	928 ± 82[a]	4.1 ± 0.2[b]
5Y	42 ± 4	58 ± 4	0.53 ± 0.03	12.8 ± 0.3[a]	200–210	534 ± 56[b]	3.2 ± 0.2[c]
LS_2	70% LS_2 crystal filled (silicate) glass		1.72 ± 0.12 (Length) 4.06 ± 0.36 (aspect ratio)	5.6 ± 0.1[b]	100–110	~400	3.0 ± 0.2[c]
Steatite	Magnesium silicate		–	4.0 ± 0.2[c]	~107[3]	~131[3]	–

Different superscripts (for each variable) indicate statistically different results (significance level $\alpha = 0.05$).
[1]Values were reported elsewhere for the same samples [5,6,61].
[2]Hardness measured using a 10-kg indentation load.
[3]Values provided by the steatite ball manufacturer (CeramTec, Germany).

Table 2 – The wear test parameters used in this study with corresponding to test configuration in Fig. 2.

Bath temperature	90 °C
Environment	Distilled water
Weight	2 kg
Circle diameter (a)	3 mm
Length of contact line (b)	2.83 mm
Intrusion depth (c)	1 mm
Speed of horizontal (d) and vertical (e) axis	20 mm/s
Cycle preset	1,200,000
Cycle frequency	2.1 Hz

using Geomagic Control X (3D-Systems, Rock Hill, South Carolina).

Wear morphologies were examined by light optical microscopy (Axioskop 40 Pol, Carl Zeiss, Oberkochen, Germany) and Scanning Electron Microscopy (SEM; Supra 40, Carl Zeiss, and FEI-Nova Nanosem 450, FEI, Eindhoven, The Netherlands). The specimens were ultrasonically cleaned in ethanol before microscopic examination without any surface treatments nor conductive layer coating.

In order to assess whether the wear environment had an influence on the surface mechanical properties of the ceramics, the surface hardness of the ceramics after the wear tests was evaluated by performing Vickers indentations at the lowest load of 0.3 kg. Ten indentations were applied on the unworn area of the ceramic that underwent wear tests; size and morphology of the indentation imprints were compared with those obtained from the pristine surface.

Phase transformations of the zirconia specimens after the wear tests were examined by X-ray diffraction (XRD; 3003-TT, Seifert, Ahrensburg, Germany) and micro-Raman spectroscopy (Senterra, BrukerOptik, Ettlingen, Germany). The XRD patterns were collected using Cu-Kα radiation at 40 kV and 40 mA from 20-90° (2θ) with a step size of 0.01 for 3 s. The monoclinic zirconia phase (*m*-ZrO_2) content was calculated according to the formula of Garvie et al. [45] that was modified by Toraya et al. [46]. Micro-Raman spectroscopy was performed using a 532-nm wavelength Ar-ion laser source through a 100x objective with a pinhole aperture of 25 μm (spot size of about 1 μm) in three successive measurements of 20 s integration time per measurement. At least 100 spots were assessed for each worn and unworn area. Depth profiles were collected from the top 15-μm surface of the worn area using confocal micro-Raman spectroscopy to analyze the subsurface phase transformation and the potential residual stresses induced by sliding wear. The micro-Raman depth spectra were collected from the surface towards the subsurface at a step size of 2 μm using a 100x objective with a pinhole aperture of 25 μm. The micro-Raman *m*-ZrO_2 fraction was calculated according to the formula of Tabares et al. [47]. For stress analysis, the Raman wavenumber of the tetragonal zirconia (t-ZrO_2) band around 147 cm^{-1} was traced using curve fitting software (fityk 1.2.1, Marcin Wojdyr, Warsaw, Poland) [48,49].

2.4. *Statistical analysis*

Statistical analysis was performed at a significance level of $\alpha = 0.05$ (Minitab® 16.2.1, Minitab, Pennsylvania, USA). One-way analysis of variance (ANOVA) followed by Tukey's post hoc cor-

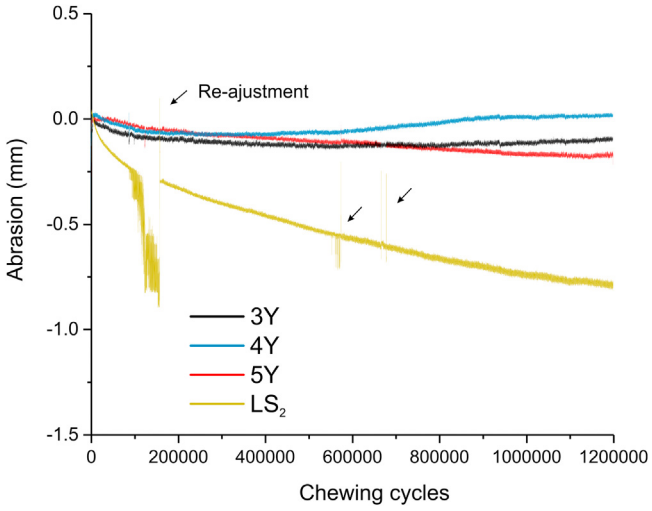

Fig. 3 – Wear history recorded from the chewing simulator.

rection was used to investigate statistical differences between mean values for hardness, roughness and wear losses.

3. Results

3.1. *Surface roughness*

All investigated ceramics allowed to obtain smooth surfaces ($R_a \leq 0.1\,\mu m$ and $R_z \leq 0.5\,\mu m$) via mechanical polishing (Table 3). ANOVA analysis showed no significant differences between the mean surface roughness (R_a and R_z) of the ceramic surfaces prior to the wear test (pristine surface; $p > 0.5$). After the wear test, the worn surface of LS_2 was significantly rougher than that of the zirconia ceramics (Table 3).

3.2. *Total abrasion*

The progressive total abrasions, i.e. intrusion depth recorded by the chewing simulator including both antagonist and ceramic, are presented in Fig. 3. The LS_2 system obviously experienced a substantially higher total abrasion than the zirconia ceramics. Due to the high wear loss of LS_2, several re-adjustments of the antagonist intrusion depth needed to be performed during the wear test, as marked by the arrows in the curves. No major abrasion was visible in the zirconia ceramics (3Y, 4Y and 5Y). Noteworthy is that although the embedding material (Technovit 4000) was designed to have minimal expansion and shrinkage, the slightly 'negative' abrasion as observed in the average plot (especially in 4Y zirconia) could be the result of a potentially slight and progressive expansion of the embedding material in water set at 90 °C. Nevertheless, the results shown hereafter were not influenced by this minor effect.

3.3. *Wear on ceramics*

The 3D-wear tracks on the ceramic surfaces along with the depth profiles recorded at the center of the wear track after 1.2 million wear cycles are shown in Fig. 4. The 'ceramic wear'

Table 3 – Surface roughness (μm), wear depth (μm), wear area (mm^2), volume loss (mm^3), and phase transformation (vol%) induced by the wear test. Average ± standard deviation is reported.

	Roughness of ceramics (μm)				Ceramic wear			Steatite antagonist wear		Monoclinic zirconia content after wear test (vol%)	
	Pristine surface		Worn area		Maximum depth (μm)	Area (mm^2)	Volume (mm^3)	Area (mm^2)	Volume (mm^3)	Worn area	Unworn area
	R_a	R_z	R_a	R_z							
3Y	0.1 ± 0.0^{a}	0.4 ± 0.1^{a}	0.11 ± 0.0^{a}	0.8 ± 0.3^{a}	10 ± 3^{a}	9 ± 2^{a}	-*	4.1 ± 1.8^{a}	0.5 ± 0.3^{a}	3.7 ± 1.2	0.24 ± 1.35
4Y	0.1 ± 0.0^{ab}	0.4 ± 0.1^{ab}	0.1 ± 0.1^{a}	0.5 ± 0.3^{a}	11 ± 10^{a}	7 ± 1^{a}	-*	3.3 ± 1.0^{a}	0.3 ± 0.1^{a}	1.5 ± 1.1	0.05 ± 0.30
5Y	0.1 ± 0.0^{ab}	0.4 ± 0.0^{bc}	0.3 ± 0.0^{a}	1.3 ± 0.8^{a}	8 ± 2^{a}	9 ± 3^{a}	-*	4.6 ± 1.7^{a}	0.6 ± 0.4^{a}	0	0
LS_2	0.1 ± 0.0^{b}	0.5 ± 0.0^{c}	1.0 ± 0.4^{b}	4.6 ± 6.7^{b}	880 ± 97^{b}	25 ± 3^{b}	12 ± 2	24 ± 4.8^{b}	3.3 ± 0.5^{b}	–	–

Different superscripts (within column) indicate significantly different experimental groups for each respective variable ($\alpha = 0.05$). (*) The very shallow wear depths did not allow an accurate quantification of the wear volume.

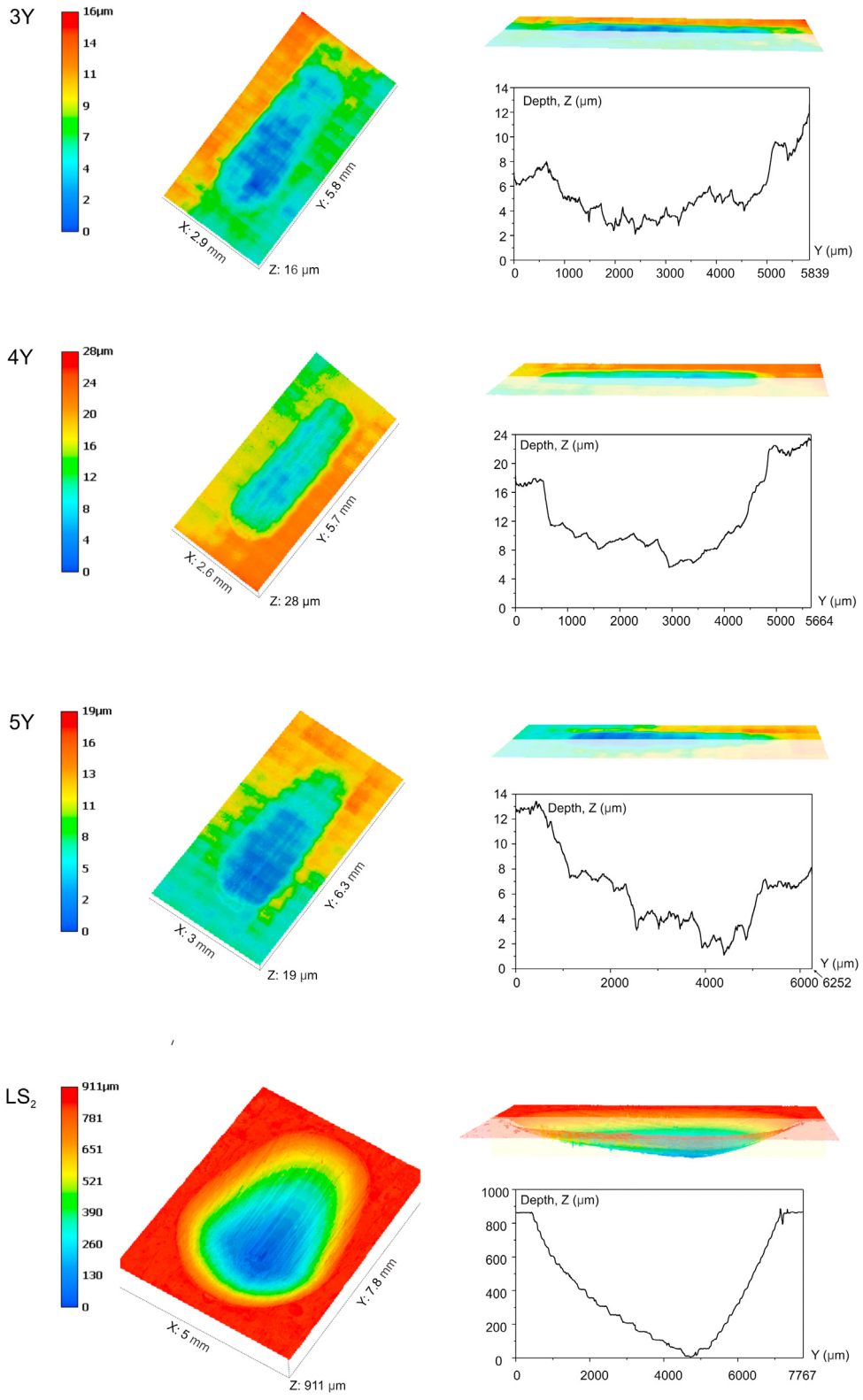

Fig. 4 – Representative scans of the wear tracks of the four ceramics after 1.2 x 10^6 wear cycles. Three-dimensional maps of the wear tracks with top and side view along with depth profiles at the center of the wear track. The scale was different for each material.

data are averaged in Table 3. Wear was detected on all the ceramics investigated, but LS_2 experienced much more severe wear than the zirconia ceramics regarding maximum wear depth and wear area. The wear volume of LS_2 was 12 ± 2 mm^3, whereas the very shallow wear depths on the zirconia ceramics did not allow an accurate quantification of the wear volumes. Independent of the yttria stabilizer content and the concomitant variation of the mechanical properties, as mentioned in Table 1, all three zirconia ceramics revealed a very limited amount of wear (~10 μm maximum wear depth on a ~10 mm^2 wear area after 1.2 million cycles); no statistical differences among the zirconia ceramics were noted for wear depth and area (Table 3).

Fig. 5 shows the wear track morphology captured from the center of the wear tracks at different magnifications. All ceramics showed a rough surface with grooves oriented parallel with the sliding direction, indicating an abrasive wear mechanism, whereas the groove sizes were different with much larger and deeper groves observed for LS_2 (see image comparisons at low magnification with a 50-μm scale bar). The images at higher magnification revealed wear pits associated with the dislodgment of ceramic particles on the worn surfaces of the zirconia ceramics. Since the grain sizes were different for the three zirconia ceramics (Fig. 1), the pit sizes were different. Cracks were not clearly observed in all zirconia ceramics, but cracks running parallel with the sliding direction were found in the wear grooves of LS_2 (Fig. 5d).

3.4. *Antagonist wear*

The three different zirconia ceramics caused a similar wear loss in area and volume on the opposing steatite antagonists (~ 4 mm^2 and <0.6 mm^3, respectively), whereas the LS_2 resulted in a significantly higher antagonist wear area of 24 ± 4.8 mm^2 and wear volume of 3.3 ± 0.5 mm^3 after 1.2 million wear cycles (Table 3). Microscopy characterization showed that the antagonists opposing the zirconia ceramics were flattened and that the worn surface was relatively smooth without chippings, cracks and deep ploughing marks (Fig. 6). In contrast, the worn surface on the LS_2 antagonists was large and covered with deep ploughing grooves.

3.5. *Phase transformation after wear test*

XRD revealed that the wear test consisting of 1.2 million cyclic chewing simultaneous with hydrothermal aging in 90 °C water for 160 h induced tetragonal (*t*-ZrO_2) to monoclinic (*m*-ZrO_2) phase transformation at the surface of 3Y and 4Y zirconia ceramics, while no monoclinic phase was observed in 5Y (Fig. S1 in supplementary figures). All zirconia ceramics after the wear test also showed a broadened (101) tetragonal peak (arrows in Fig. S1 a), which indicated the presence of rhombohedral zirconia phase or sometimes named as distorted tetragonal zirconia [50,51]. On the other hand, the phase composition of LS_2 remained the same before and after wear testing (also confirmed by micro-Raman spectroscopy) (Fig. S1 b). The scanned XRD area covered both worn and unworn regions (as illustrated schematically in Fig. S1). Micro-Raman spectroscopy was thus complementarily used to locally evaluate phase transformation (lateral resolution of 1 μm) in order to distinguish between the contribution from the cyclic loading and the water environment (Fig. 7). The measurements in the unworn area revealed that water at 90 °C induced a very limited amount of *t*-*m* phase transformation (on average 0.24 ± 1.35 and 0.05 ± 0.30 vol% of *m*-ZrO_2 for 3Y for 4Y, respectively; Table 3), but the transformed zirconia was not homogenously distributed (some spots were free of *m*-ZrO_2, while other spots were transformed (Fig. 7a). Higher but still modest amounts of *m*-ZrO_2 were detected in the worn areas (3.7 ± 1.2 vol% for 3Y and 1.5 ± 1.1 vol% for 4Y; Table 3); spots free of *m*-ZrO_2 were not detected in the worn areas, showing that both cyclic loading and water environment contributed to the phase transformation during the wear process. Again, no transformation was observed in both unworn and worn areas of 5Y. Depth analysis using confocal micro-Raman spectroscopy showed that the transformations in the worn area took place up to about 10 μm and 6 μm deep into the 3Y and 4Y zirconia ceramics, respectively (Fig. 7b). In addition, a clear peak shift towards a higher wavelength was observed in the worn areas of all zirconia ceramics (Fig. 7c).

3.6. *Surface hardness*

Fig. 8 displays the 0.3-kg Vickers indentations performed in the unworn area of the samples that underwent the wear test as compared to the surface hardness measured before the wear test in the pristine surface, this is to assess whether the wear environment (90 °C water) had an influence on the surface hardness of the investigated ceramics and to analyze the surface corrosion effects. No difference was observed for the three zirconia ceramics before and after the wear test (the same indentation imprints, crack patterns and $HV_{0.3}$ hardness values of ~14 GPa). However, the surface of LS_2 was clearly softened by the 90 °C water environment during the wear test. The edge of the indent was less sharp and chipped, which made quantification of hardness less accurate. A rough estimation revealed a lower $HV_{0.3}$ hardness of 4.5 ± 0.4 GPa for LS_2 after the wear test, as compared to an initial $HV_{0.3}$ of 5.9 ± 0.7 GPa (before the wear test).

4. Discussion

The hypothesis of this study that the high-translucent zirconia ceramics stabilized with higher yttria contents would show a different wear behavior than 3Y-TZP ceramics due to different fracture toughness and aging susceptibility failed to be accepted. It has well been documented that hardness solely is not reliable to predict wear behavior of ceramic materials; there is no strong correlation between ceramic hardness and wear of opposing dentition [12,14,37]. This is because wear of intrinsically brittle ceramics occurs by fracture rather than by plastic deformation [52,53], while hardness is a measure of resistance to localized plastic deformation. Alternatively, fracture toughness was emphasized in earlier reports for the wear resistance of brittle ceramics [12,17,33,37,54], being the basis of the null hypothesis advanced in this study. However, the present study showed that, independent of fracture toughness, strength (Table 1) and aging susceptibility (Fig. 7), the zirconia ceramics stabilized with 3, 4 and 5 mol% yttria (3Y, 4Y

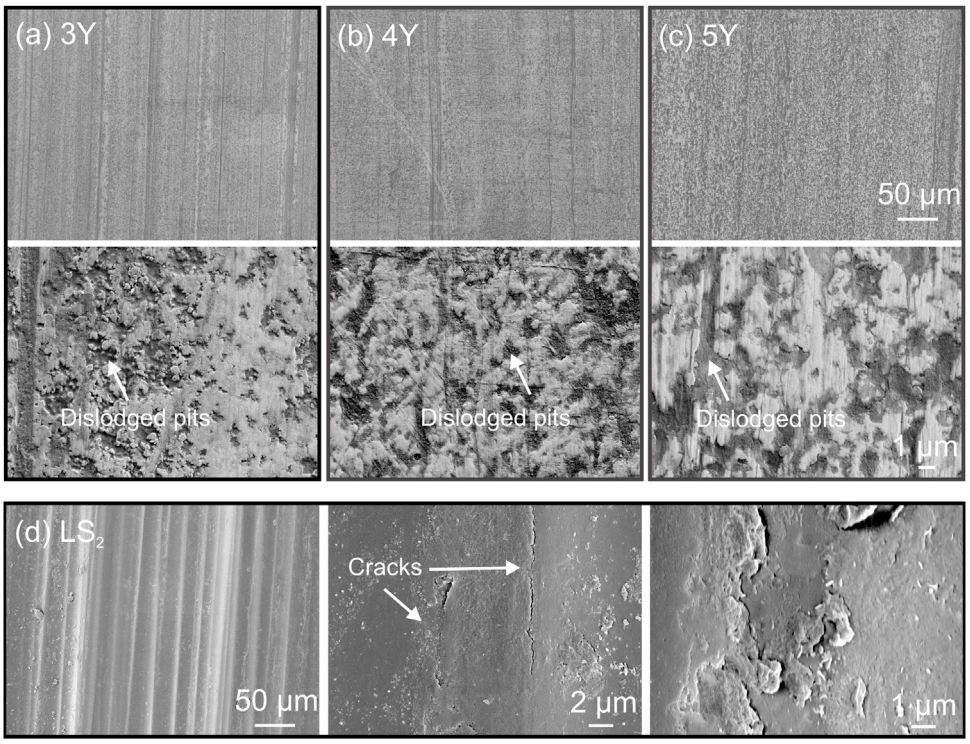

Fig. 5 – SEM images of the center of the wear crater at two magnifications for the three zirconia ceramics (a–c) and at three magnifications for LS_2 (d). The high magnification images for LS_2 were captured at different scales to better illustrate the wear features.

and 5Y) gave rise to a high wear resistance and a comparably low steatite antagonist wear (Table 3, Fig. 4). Moreover, LS_2, having a similar fracture toughness as 5Y, showed a higher ceramic and antagonist wear (Table 3, Figs. 3, 4 and 6). The combination of hardness and toughness therefore was not enough to predict the wear behavior of dental ceramics.

4.1. *Wear of zirconia ceramics*

Fracture toughness is a measure of the resistance to crack propagation, so it should be determining when crack formation and propagation, and surface chipping or fracture are involved in the wear processes, as documented for glass-ceramics, glass-infiltrated ceramics, feldspar ceramics, etc. [12,14,15,17–19,31,33–37]. However, for the zirconia ceramics studied in this work, abrasive wear with grain pullouts was found to be the principal wear mechanism; no (micro-)cracks and/or chipping flakes were identified in their wear tracks (Fig. 5), in agreement with previous studies on monolithic dental 3Y-TZP ceramics [13–19]. It is therefore logical to find that wear behavior of the investigated zirconia ceramic was similar, independent of their different fracture toughness and other crack-related properties like R-curve behavior. It is important to note that the wear mechanism of ceramic materials and the concomitant wear behavior are highly dependent on the wear test conditions, which means that the dependence of zirconia's wear resistance on fracture toughness could differ depending on the wear conditions. For example, micro-cracks are easily formed during wear of zirconia ceramics in a dry or low humidity condition (although less relevant for den-

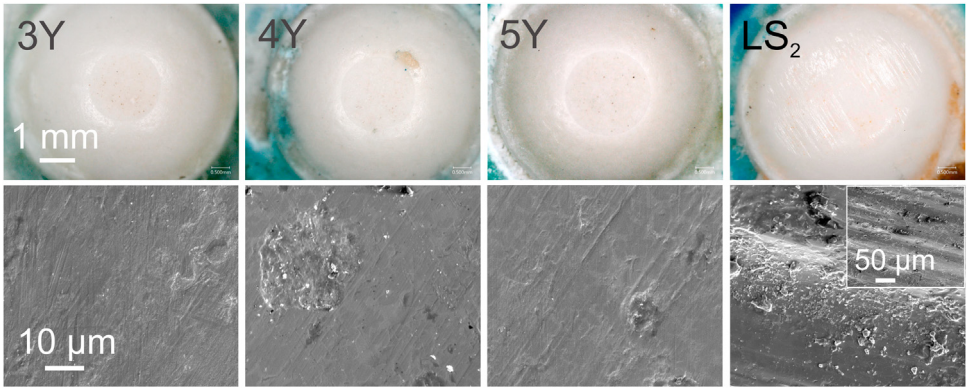

Fig. 6 – Optical microscopy and SEM images of the steatite antagonist against the 3Y, 4Y, 5Y and LS_2 ceramics.

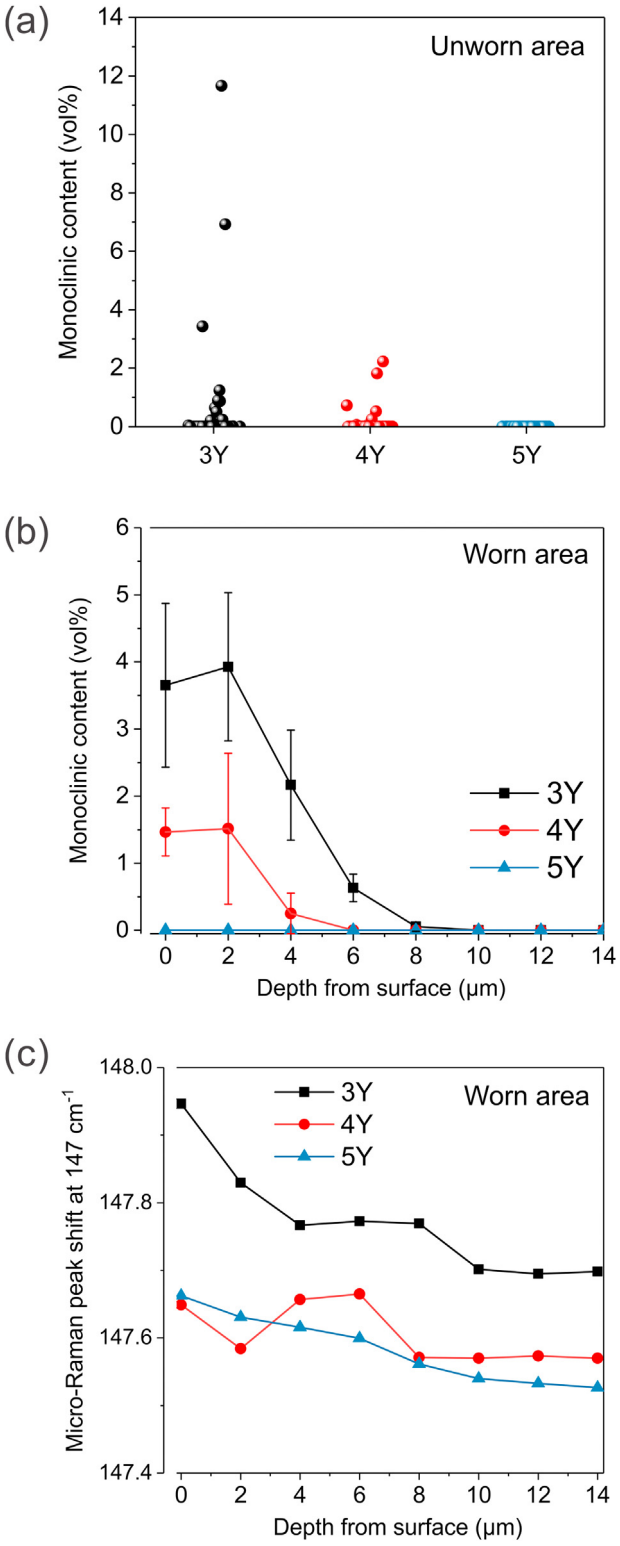

Fig. 7 – Micro-Raman investigations of zirconia samples after wear testing: (a) Individual plot of monoclinic phase content detected on the unworn area (>100 date points for each material) with average monoclinic content of 0.24 ± 1.35 and 0.05 ± 0.30 vol% for 3Y for 4Y, respectively. (b) Monoclinic phase content in the worn area as a function of the depth from the surface. (c) t-ZrO_2 peak position as a function of depth from the worn surface in accompaniment corresponding to the data points in Fig. 7b.

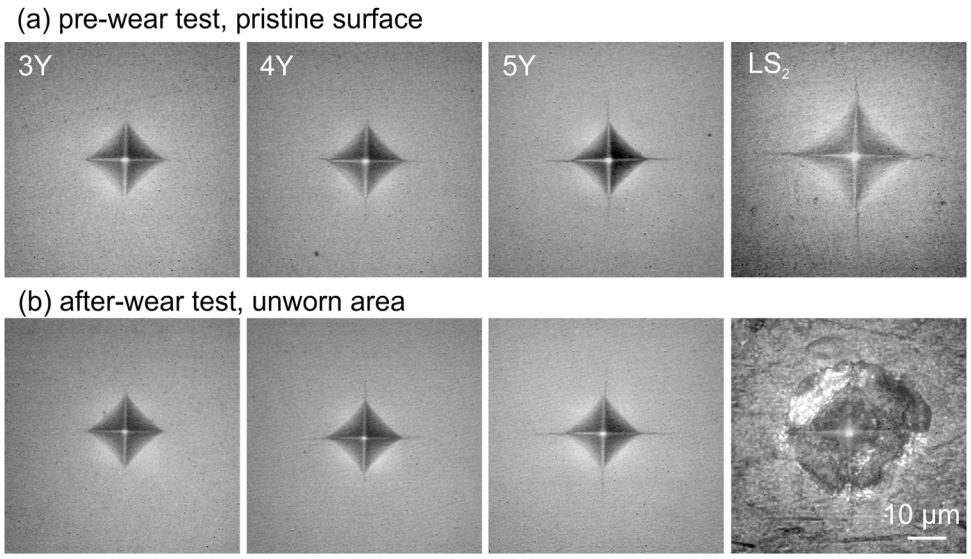

Fig. 8 – Surface hardness using 0.3 kg Vickers indentations before and after wear testing: (a) Indentation imprints obtained from the pristine surfaces; (b) Imprints obtained from the unworn area of the specimens after wear testing, showing the effect of the water environment.

tal applications), in which zirconia ceramics stabilized with a higher yttria content, having resulted in a higher cubic content and lower fracture toughness, indeed revealed a faster wear rate [33]. Wear mechanism can be transitioned under different loads as well. As observed for leucite glass-ceramics and feldspar ceramics [12,55], low contact loads are associated with abrasive wear and low friction, whereas high contact loads and high friction can lead to the formation of microcracks or even delamination wear. One study suggested that the wear mechanism of 3Y-TZP transitioned to micro-cracking at sliding loads above 20 N under steel ball counterpart of 10 mm in diameter [56]. The load applied in chewing simulators varies between 5 and 100 N [14,57] and considering the fact that zirconia can be suggested for load-bearing areas, further research is needed to assess wear behavior of these new high-translucent zirconia ceramics under higher chewing loads.

4.2. *Wear resistance of LS_2 versus that of zirconia ceramics*

The lower wear resistance of LS_2 in comparison to all zirconia ceramics is not only related to its lower hardness (Table 1), but should also be attributed to its higher susceptibility to slow crack growth (stress-corrosion) and lower fatigue threshold [6] (fatigue wear) and surface corrosion (corrosion wear) (Fig. 8). As discussed earlier in section 4.1, fracture toughness can be a key parameter in the ceramic wear process when crack formation is present [12,33,37,58]. Cracks were clearly observed in the worn area of LS_2 (Fig. 5b), but LS_2 and 5Y having a similar fracture toughness and strength (Table 1) [6,59] still showed different wear behaviors. This highlights the importance of other factors in addition to the fracture toughness and we believe that the fatigue threshold was a vital parameter to understand the wear behavior of LS_2 in comparison to 5Y. Fracture toughness (K_{IC}) defines the critical stress-intensity factor, i.e. resistance to fast crack propagation, but the crack growth occurs at stress-intensity levels (K_I) below the critical stress-intensity factor, i.e. slow crack-growth (SCG) behavior [60]. The importance of the SCG behavior and threshold stress-intensity factor below which no slow crack growth occurs, has been emphasized for the loading-bearing capacity of dental ceramics [12,53,61,62], but not for their wear performance. Our recent work on the fatigue behavior of the four materials studied herein showed that LS_2 was more susceptible to water-assisted SCG with a smaller stress-corrosion coefficient parameter and lower threshold for fatigue-crack growth (K_{I0} of about 1.0 MPa $m^{1/2}$), as compared to 5Y zirconia with a fatigue threshold of 1.4 MPa $m^{1/2}$ (40% higher) [6]. As such, it can be expected that relative to zirconia ceramics, defects or contact damages in LS_2 start to grow at a lower chewing load, or that under the same load, crack propagation is faster and a relatively lower number of cycles are needed to cause chipping and fracture. Indeed, subsurface cracks were observed in the wear grooves of LS_2 but not in the zirconia ceramics, including 5Y (Fig. 5). Furthermore, the cracks and detached wear particles (Fig. 5d) in LS_2 were found to run parallel with the sliding direction, confirming the effect of the cyclic tensile load on the lateral crack extension by the sliding antagonist, i.e. fatigue wear. This finding agrees with earlier work, showing that fatigue wear flakes and even delamination wear were observed for lithium-disilicate glass ceramic at relatively low chewing loads of 5–25 N [63].

Importantly, LS_2 suffered from surface degradation in an aqueous environment and a surface-hardness drop after wear testing (Fig. 8). LS_2 consists of 70 vol% $Li_2Si_2O_5$ crystals and 30 vol% of a silicate glass phase. Dissolution of Si-O-Si glass network in an aqueous environment is a well-known phenomenon [37,64], which generally results in a hydrated layer depleted of the soluble species and softens the surface of glass-containing ceramics [64]. The severity of the dissolution depends on the glass composition, pH and reaction temperature. At the present study performed at 90 °C water,

the surface dissolution and the concomitant ion leaching with the formation of soft hydrated silica layer would be enhanced, contributing to a greater plowing wear in LS_2. No clear indication was found in the literature for the dissolution of crystalline ceramics including alumina and zirconia in an aqueous environment [64,65]. A concern to the surface degradation of zirconia ceramics could lie in their susceptibility to hydrothermal aging in a water environment, which could degrade their surface hardness and elastic modulus due to spontaneous *t-m* phase transformation and the formation of micro-cracks in the subsurface [66]. This however was not observed in the present study. 5Y was aging-resistant under the current experimental conditions (Fig. 7a), in agreement with earlier studies using accelerated aging test in water at 134 °C [10]. Although 3Y and 4Y were susceptible to aqueous aging and indeed showed phase transformation (Fig. 7a), their surface hardness was not influenced (Fig. 8). The distribution of aging-induced monoclinic zirconia in 3Y and 4Y was non-homogeneous with some 1-μm micro-Raman spots being free of *m*-ZrO_2 (Fig. 7a). This indicates that the kinetics of hydrothermal aging in 3Y and 4Y after the wear test corresponded to the very early nucleation stage of monoclinic phase formation at isolated surface grains [67,68]. In this early stage, micro-cracks are generally not formed and a decrease in hardness is not observed [39,66]. Furthermore, compressive stress was recorded in the worn area of zirconia ceramics (Fig. 7c), for which crack formation and extension should not be promoted.

4.3. *Antagonist wear*

The low antagonist wear recorded for 4Y and 5Y was in line with the behavior of 3Y and earlier reports showing that the high hardness of zirconia ceramics does not have detrimental consequences on wear of the opposing counterfaces [13,14,17]. The antagonist wear against ceramics is reported not to be directly related to their hardness, but to depend more on their microstructure (phases homogeneity and porosity). Also, the surface roughness developed on the worn ceramic surface was found to play a crucial role [14,15,17,18,26–28]. All the zirconia ceramics investigated reached a smooth surface after adequate polishing (Table 3) and, more importantly, due to their high wear resistance and dense microstructure, the contacting surfaces could remain relatively smooth during wear (Fig. 5), having resulted in reduced friction with the opposing antagonist. Although the size of the pull-out grains and dislodged pits were different, the surface roughness of all worn zirconia ceramic surfaces was comparable (Table 3). Coupling hydrothermal aging of the zirconia ceramics (water at 90 °C) did not influence the antagonist wear (Fig. 6). As discussed in section 4.2, aging of 3Y and 4Y (5Y was aging-free) was limited to the very early stage of transformation nucleation, whereas significant surface roughening is normally only recorded in a later stage through extensive growth of transforming monoclinic phase [41,69]. In fact, no studies in restorative dentistry following clinical investigations or simulated aging (at 5–55 °C or autoclaving at 135 °C) [14,15,18,70] have reported the issue of aging susceptibility of zirconia ceramics on wear of an opposing antagonist or enamel.

The higher antagonist wear of LS_2 than recorded for the zirconia ceramics is in agreement with many other observations of wear against both steatite and enamel antagonists [13,34,57,71]. A high surface roughness (Table 3) is known to increase friction at the interface, which not only causes a higher abrasive action on the opposing antagonist but also reduces the resistance to sliding contact and in turn increases the fracture and wear rate of the ceramic material itself [54]. The worn surfaces of LS_2 in Figs. 5 and 6 showed that the size of the grooves on both the ceramic and antagonist surface were deep and large, indicating the rather severe abrasiveness of both counterparts to each other. Moreover, unlike zirconia ceramics, the microstructure of LS_2 is non-homogeneous with mixed glass, hard crystals and porosity (Fig. 1). The glass phase in LS_2 is known to be susceptible to fast dissolution in an aqueous environment, while the dissolution of the $Li_2Si_2O_5$ occurs slowly enhancing surface roughness and exposing the sharp and hard crystals to the antagonist material [64,72]. In order to examine the solubility of the four ceramics studied, they have been submitted to 16 -h acid etching test in 4% acetic acid at 80 °C following the ISO 6872 standard. The results showed that the glass phase in LS_2 indeed dissolved at a faster rate than the $Li_2Si_2O_5$ crystals, resulting in the exposure/pull-out of crystals on the etched surface (Fig. S2 in the supplementary figures). Similarly, pores exposed to the wear process produce sharp edges and also enhance the wear rate [37].

4.4. *Clinical implications and future work*

The use of 3Y-TZP for monolithic restorations is justified when a good surface finish is achieved [13,14,17,26–30]. Therefore, 4Y and 5Y ceramics, showing a similar two-body wear behavior as 3Y, can also be considered suitable choices for dental restorations. Nevertheless, the oral environment being complex and highly varied, there are some differences between the actual application conditions and that applied in this work. The 1.2 million cycles are generally recognized to be equivalent to 5-year function in the mouth [43], but some people can chew up to 1 million cycles per year [73] and clinical wear is sometimes more dependent on the patient's chewing characteristics than on the material [74]. Temperature fluctuations are experienced in the oral environment and a water flow at 5–55 °C is normally applied to the wear test chamber simulating such intra-oral temperature fluctuations. The continuously circulated water of 90 °C applied in this study is certainly more aggressive than the oral environment, especially for LS_2 that is susceptible to aqueous dissolution and stress-corrosion (i.e. slow crack growth behavior). Similarly, there might be a difference between the surface treatments applied in this work (mirror polishing) with the ones applied in clinics. It is common knowledge that the surface must be well-polished for monolithic restorations to reduce opposing enamel wear [14,26–30,75], but good quantification of 'well' polishing is lacking. Above all, the wear test results obtained in this work cannot be directly used to predict real wear of the ceramic materials and opposing enamel in oral conditions. Actually, it is difficult or even impossible to simulate clinical wear using *in-vitro* studies. Nevertheless, *in-vitro* experiments allow to evaluate the effect of specific variables and to predict the behavior of materials, hereby aiding in the

understanding of the underlying wear mechanisms, assisting the development of new materials and elucidating some important criteria for material selection, as has been the main purpose of this work.

Some further investigations are needed to elucidate the wear behavior of 4Y and 5Y in a condition that is more closely resembling to the oral cavity, such as a higher chewing load in an environment with varied pH values, using 3-body wear testing and CAD/CAM machined specimens. Human enamel cusps can be used as antagonist as well, since steatite cannot accurately mimic the complex enamel structure. However, it may be difficult to standardize specimens when using human enamel cusps due to the huge discrepancy in teeth mineralization, cusps anatomy and micro-morphology; this variation can be expected to give rise to large deviations in antagonist wear compared to the use of ceramic cusps [57]. Steatite spheres have a hardness and friction similar to that of enamel [76] and thus were used here, representing a soft antagonist. There may however be clinical conditions, in which a ceramic restoration may act as antagonist, by which the wear mechanism against a hard antagonist, like zirconia or alumina, can be expected to be different as compared to an enamel antagonist [17,34]. Further research using a zirconia antagonist is therefore required.

5. Conclusions

Under the experimental conditions applied in this study, the wear behavior of zirconia ceramics stabilized with 3, 4 or 5 mol% yttria was similar and low wear for both the ceramic and steatite antagonist were recorded. Distinct wear mechanisms were observed for polycrystalline zirconia ceramics and lithium-disilicate glass-ceramic (abrasion for all investigated zirconia while abrasion, fatigue and corrosion for glass-ceramic), the latter thus having resulted in a more severe ceramic wear and enhanced abrasiveness towards the antagonist. Furthermore, the combination of hardness and fracture toughness was insufficient to predict the relative wear behavior of ceramic materials. The threshold in stress intensity for crack growth along with the microstructural homogeneity and surface degradation are also key parameters that should be taken into account in the analysis of wear behaviour.

Acknowledgements

F. Zhang thanks Research Foundation - Flanders (FWO Vlaanderen) for her post-doctoral fellowship (12S8418N). We thank Ivoclar Vivadent for providing the IPS e.max CAD ceramics (HT, A2/B40 L). Christiane Schöpf is highly acknowledged for performing the roughness measurements and Uz Hetzelberger is likewise acknowledged for embedding the samples for the chewing simulator.

Appendix A. Supplementary data

Supplementary material related to this article can be found, in the online version, at doi:https://doi.org/10.1016/j.dental.2019.10.009.

REFERENCES

[1] Piconi C, Maccauro G. Zirconia as a ceramic biomaterial. Biomaterials 1999;20:1–25.
[2] Denry I, Kelly JR. State of the art of zirconia for dental applications. Dent Mater 2008;24:299–307.
[3] Hannink RHJ, Kelly PM, Muddle BC. Transformation toughening in zirconia-containing ceramics. J Am Ceram Soc 2000;83:461–87.
[4] SWAIN MV, ROSE LRF. Strength limitations of transformation-toughened zirconia alloys. J Am Ceram Soc 1986;69:511–8.
[5] Zhang Y, Lawn BR. Novel zirconia materials in dentistry. J Dent Res 2018;97:140–7.
[6] Zhang F, Reveron H, Spies BC, Van Meerbeek B, Chevalier J. Trade-off between fracture resistance and translucency of zirconia and lithium-disilicate glass ceramics for monolithic restorations. Acta Biomater 2019;91:24–34.
[7] Denry I, Kelly JR. Emerging ceramic-based materials for dentistry. J Dent Res 2014;93:1235–42.
[8] Inokoshi M, Pongprueksa P, De Munck J, Zhang F, Vanmeensel K, Minakuchi S, et al. Influence of light irradiation through zirconia on the degree of conversion of composite cements. J Adhesive Dent 2016;18:161–71.
[9] Koch A, Kroeger M, Hartung M, Manetsberger I, Hiller KA, Schmalz G, et al. Influence of ceramic translucency on curing efficacy of different light-curing units. J Adhesive Dent 2007;9:449–62.
[10] Zhang F, Inokoshi M, Batuk M, Hadermann J, Naert I, Van Meerbeek B, et al. Strength, toughness and aging stability of highly-translucent Y-TZP ceramics for dental restorations. Dent Mater 2016;32:e327–37.
[11] Zhang Y. Making yttria-stabilized tetragonal zirconia translucent. Dent Mater 2014;30:1195–203.
[12] Kruzic JJ, Arsecularatne JA, Tanaka CB, Hoffman MJ, Cesar PF. Recent advances in understanding the fatigue and wear behavior of dental composites and ceramics. J Mechanical Behav Biomed Mater 2018;88:504–33.
[13] Kim MJ, Oh SH, Kim JH, Ju SW, Seo DG, Jun SH, et al. Wear evaluation of the human enamel opposing different Y-TZP dental ceramics and other porcelains. J Dent 2012;40:979–88.
[14] Miyazaki T, Nakamura T, Matsumura H, Ban S, Kobayashi T. Current status of zirconia restoration. J Prosthodontic Res 2013;57:236–61.
[15] Rosentritt M, Preis V, Behr M, Hahnel S, Handel G, Kolbeck C. Two-body wear of dental porcelain and substructure oxide ceramics. Clin Oral Investigations 2012;16:935–43.
[16] Bano S, Kaizer MR, Dos Santos MBF, Zhang Y. Wear and fatigue behavior of monolithic zirconia crown restorations. Dent Mater 2017;33:e9.
[17] Albashaireh ZSM, Ghazal M, Kern M. Two-body wear of different ceramic materials opposed to zirconia ceramic. J Prosthetic Dent 2010;104:105–13.
[18] Preis V, Behr M, Kolbeck C, Hahnel S, Handel G, Rosentritt M. Wear performance of substructure ceramics and veneering porcelains. Dent Mater 2011;27:796–804.
[19] Mormann WH, Stawarczyk B, Ender A, Sener B, Attin T, Mehl A. Wear characteristics of current aesthetic dental restorative CAD/CAM materials: two-body wear, gloss retention, roughness and Martens hardness. J Mechanical Behav Biomed Mater 2013;20:113–25.
[20] Pathan MS, Kheur MG, Patankar AH, Kheur SM. Assessment of antagonist enamel wear and clinical performance of full-contour monolithic zirconia crowns: one-year results of a prospective study. J Prosthodontics 2019;28:e411–6.
[21] Lohbauer U, Reich S. Antagonist wear of monolithic zirconia crowns after 2 years. Clin Oral Investig 2017;21:1165–72.

[22] Esquivel-Upshaw JF, Kim MJ, Hsu SM, Abdulhameed N, Jenkins R, Neal D, et al. Randomized clinical study of wear of enamel antagonists against polished monolithic zirconia crowns. J Dent 2018;68:19–27.
[23] Tambra T, Razzoog M, Lang B, Wang R, Lang B. Wear of enamel opposing YPSZ zirconia core material with two surface finish. In: 32nd AADR; 2003.
[24] Culver S, Cakir D, Burgess J, Ramp L. Wear of the enamel antagonist and five restorative materials. In: 37th AADR; 2008.
[25] Shar S, Mickelson C, Beck P, Lamp L, Cakir D, Burgess J. Wear of enamel on polished and glazed zirconia. In: 39th AADR; 2010 [Abstr No 227].
[26] Lawson NC, Janyavula S, Syklawer S, McLaren EA, Burgess JO. Wear of enamel opposing zirconia and lithium disilicate after adjustment, polishing and glazing. J Dent 2014;42:1586–91.
[27] Stawarczyk B, Ozcan M, Schmutz F, Trottmann A, Roos M, Hammerle CH. Two-body wear of monolithic, veneered and glazed zirconia and their corresponding enamel antagonists. Acta Odontol Scand 2013;71:102–12.
[28] Janyavula S, Lawson N, Cakir D, Beck P, Ramp LC, Burgess JO. The wear of polished and glazed zirconia against enamel. J Prosthetic Dent 2013;109:22–9.
[29] Preis V, Grumser K, Schneider-Feyrer S, Behr M, Rosentritt M. Cycle-dependent in vitro wear performance of dental ceramics after clinical surface treatments. J Mech Behav Biomed Mater 2016;53:49–58.
[30] Preis V, Behr M, Handel G, Schneider-Feyrer S, Hahnel S, Rosentritt M. Wear performance of dental ceramics after grinding and polishing treatments. J Mech Behav Biomed Mater 2012;10:13–22.
[31] Borrero-Lopez O, Guiberteau F, Zhang Y, Lawn BR. Wear of ceramic-based dental materials. J Mech Behav Biomed Mater 2019;92:144–51.
[32] Basu B, Vleugels J, Van Der Biest O. Microstructure–toughness–wear relationship of tetragonal zirconia ceramics. J Eur Ceramic Soc 2004;24:2031–40.
[33] Fischer TE, Anderson MP, Jahanmir S. Influence of fracture toughness on the wear resistance of yttria-doped zirconium oxide. J Am Ceram Soc 1989;72:252–7.
[34] Dupriez ND, von Koeckritz AK, Kunzelmann KH. A comparative study of sliding wear of nonmetallic dental restorative materials with emphasis on micromechanical wear mechanisms. J Biomed Mater Res B Appl Biomater 2015;103:925–34.
[35] Truong V-T, Cock DJ, Padmanathan N. Fatigue crack propagation in posterior dental composites and prediction of clinical wear. J Appl Biomater 1990;1:21–30.
[36] Santos F, Branco A, Polido M, Serro AP, Figueiredo-Pina CG. Comparative study of the wear of the pair human teeth/Vita Enamic(R) vs commonly used dental ceramics through chewing simulation. J Mech Behav Biomed Mater 2018;88:251–60.
[37] Oh WS, Delong R, Anusavice KJ. Factors affecting enamel and ceramic wear: a literature review. J Prosthetic Dent 2002;87:451–9.
[38] Lughi V, Sergo V. Low temperature degradation -aging- of zirconia: a critical review of the relevant aspects in dentistry. Dent Mater 2010;26:807–20.
[39] Muñoz-Tabares JA, Jiménez-Piqué E, Anglada M. Subsurface evaluation of hydrothermal degradation of zirconia. Acta Mater 2011;59:473–84.
[40] Chevalier J, Gremillard L, Virkar AV, Clarke DR. The tetragonal-monoclinic transformation in zirconia: lessons learned and future trends. J Am Ceram Soc 2009;92:1901–20.
[41] Gremillard L, Martin L, Zych L, Crosnier E, Chevalier J, Charbouillot A, et al. Combining ageing and wear to assess the durability of zirconia-based ceramic heads for total hip arthroplasty. Acta Biomater 2013;9:7545–55.
[42] Spies BC, Maass ME, Adolfsson E, Sergo V, Kiemle T, Berthold C, et al. Long-term stability of an injection-molded zirconia bone-level implant: a testing protocol considering aging kinetics and dynamic fatigue. Dent Mater 2017;33:954–65.
[43] DeLong R, Douglas WH. Development of an artificial oral environment for the testing of dental restoratives: bi-axial force and movement control. J Dent Res 1983;62:32–6.
[44] Zhang F, Inokoshi M, Vanmeensel K, Van Meerbeek B, Naert I, Vleugels J. Lifetime estimation of zirconia ceramics by linear ageing kinetics. Acta Mater 2015;92:290–8.
[45] Garvie RC, Nicholson PS. Phase analysis in zirconia systems. J Am Ceram Soc 1972;55:303–5.
[46] Toraya H, Yoshimura M, Somiya S. Calibration curve for quantitative analysis of the monoclinic-tetragonal ZrO_2 system by X-Ray diffraction. J Am Ceram Soc 1984;67. C-119-C-21.
[47] Muñoz Tabares JA, Anglada MJ. Quantitative analysis of monoclinic phase in 3Y-TZP by raman spectroscopy. J Am Ceram Soc 2010;93:1790–5.
[48] Pezzotti G, Porporati AA. Raman spectroscopic analysis of phase-transformation and stress patterns in zirconia hip joints. J Biomed Optics 2004;9:372–84.
[49] Wojdyr M. Fityk: a general-purpose peak fitting program. J Appl Crystallogr 2010;43:1126–8.
[50] Inokoshi M, Shimizu H, Nozaki K, Takagaki T, Yoshihara K, Nagaoka N, et al. Crystallographic and morphological analysis of sandblasted highly translucent dental zirconia. Dent Mater 2018;34:508–18.
[51] Hasegawa H. Rhombohedral phase produced in abraded surfaces of partially stabilized zirconia (PSZ). J Mater Sci Lett 1983;2:91–3.
[52] Mecholsky Jr JJ. Fracture mechanics principles. Dent Mater 1995;11:111–2.
[53] Zhang Y, Sailer I, Lawn BR. Fatigue of dental ceramics. J Dent 2013;41:1135–47.
[54] Ren L, Zhang Y. Sliding contact fracture of dental ceramics: principles and validation. Acta Biomater 2014;10:3243–53.
[55] Guo J, Li D, Wang H, Yang Y, Wang L, Guan D, et al. Effect of contact stress on the cycle-dependent wear behavior of ceramic restoration. J Mech Behav Biomed Mater 2017;68:16–25.
[56] Liu H, Xue Q. Wear mechanisms of zirconia/steel reciprocating sliding couple under water lubrication. Wear 1996;201:51–7.
[57] Heintze SD, Cavalleri A, Forjanic M, Zellweger G, Rousson V. Wear of ceramic and antagonist—a systematic evaluation of influencing factors in vitro. Dent Mater 2008;24:433–49.
[58] Yamamoto T, Olsson M, Hogmark S. Three-body abrasive wear of ceramic materials. Wear 1994;174:21–31.
[59] Yan J, Kaizer MR, Zhang Y. Load-bearing capacity of lithium disilicate and ultra-translucent zirconias. J Mech Behav Biomed Mater 2018;88:170–5.
[60] Lawn B. Fracture of brittle solids. second edition Cambridge: Cambridge University Press; 1993.
[61] Wendler M, Belli R, Valladares D, Petschelt A, Lohbauer U. Chairside CAD/CAM materials. Part 3: cyclic fatigue parameters and lifetime predictions. Dent Mater 2018;34:910–21.
[62] Gonzaga CC, Cesar PF, Miranda Jr WG, Yoshimura HN. Slow crack growth and reliability of dental ceramics. Dent Mater 2011;27:394–406.
[63] Peng Z, Izzat Abdul Rahman M, Zhang Y, Yin L. Wear behavior of pressable lithium disilicate glass ceramic. J Biomed Mater Res B Appl Biomater 2016;104:968–78.
[64] Swain MV. Impact of oral fluids on dental ceramics: what is the clinical relevance? Dent Mater 2014;30:33–42.

[65] Milleding P, Karlsson S, Nyborg L. On the surface elemental composition of non-corroded and corroded dental ceramic materials in vitro. J Mater Sci Mater Med 2003;14:557–66.
[66] Gaillard Y, Jiménez-Piqué E, Soldera F, Mücklich F, Anglada M. Quantification of hydrothermal degradation in zirconia by nanoindentation. Acta Mater 2008;56:4206–16.
[67] Gremillard L, Chevalier J, Epicier T, Deville S, Fantozzi G. Modeling the aging kinetics of zirconia ceramics. J Eur Ceramic Soc 2004;24:3483–9.
[68] Chevalier J, Gremillard L, Deville S. Low-temperature degradation of Zirconia and implications for biomedical implants. Ann Rev Mater Res 2007;37:1–32.
[69] Douillard T, Chevalier J, Descamps-Mandine A, Warner I, Galais Y, Whitaker P, et al. Comparative ageing behaviour of commercial, unworn and worn 3Y-TZP and zirconia-toughened alumina hip joint heads. J Eur Ceramic Soc 2012;32:1529–40.
[70] Burgess J, Janyavula S, Lawson N, Lucas T, Cakir D. Enamel wear opposing polished and aged zirconia. Oper Dent 2014;39:189–94.
[71] Nakashima J, Taira Y, Sawase T. In vitro wear of four ceramic materials and human enamel on enamel antagonist. Eur J Oral Sci 2016;124:295–300.
[72] Heintze SD, Rousson V. Survival of zirconia- and metal-supported fixed dental prostheses: a systematic review. Int J Prosthodont Restor Dent 2010;23:493–502.
[73] Po JM, Kieser JA, Gallo LM, Tesenyi AJ, Herbison P, Farella M. Time-frequency analysis of chewing activity in the natural environment. J Dent Res 2011;90:1206–10.
[74] Heintze SD, Faouzi M, Rousson V, Ozcan M. Correlation of wear in vivo and six laboratory wear methods. Dent Mater 2012;28:961–73.
[75] Mitov G, Heintze SD, Walz S, Woll K, Muecklich F, Pospiech P. Wear behavior of dental Y-TZP ceramic against natural enamel after different finishing procedures. Dent Mater 2012;28:909–18.
[76] Wassell RW, McCabe JF, Walls AW. A two-body frictional wear test. J Dent Res 1994;73:1546–53.